Study on effects of solar radiation and rain on shrinkage, shrinkage cracking and creep of concrete

Shingo Asamoto [a,*], Ayumu Ohtsuka [b], Yuta Kuwahara [c], Chikako Miura [d]

[a] Department of Civil & Environmental Engineering, Saitama University, Japan
[b] Pacific Consultants Company Limited, Japan
[c] Tokyo Metropolitan Government, Japan
[d] Tokyu Construction Company Limited, Japan

ARTICLE INFO

ABSTRACT

In this paper, the effects of actual environmental actions on shrinkage, creep and shrinkage cracking of concrete are studied comprehensively. Prismatic specimens of plain concrete were exposed to three sets of artificial outdoor conditions with or without solar radiation and rain to examine the shrinkage. For the purpose of studying shrinkage cracking behavior, prismatic concrete specimens with reinforcing steel were also subjected to the above conditions at the same time. The shrinkage behavior is described focusing on the effects of solar radiation and rain based on the moisture loss. The significant environment actions to induce shrinkage cracks are investigated from viewpoints of the amount of the shrinkage and the tensile strength. Finally, specific compressive creep behavior according to solar radiation and rainfall is discussed. It is found that rain can greatly inhibit the progresses of concrete shrinkage and creep while solar radiation is likely to promote shrinkage cracking and creep.

© 2011 Elsevier Ltd. All rights reserved.

1. Introduction

Large and long-term time-dependent deformations, such as shrinkage and creep, are exhibited by concrete, which is one of the most typical construction materials. Restraint of the shrinkage by internal reinforcement and external boundary conditions induces a tensile stress in concrete and cracks form when the stress reaches the tensile strength, reducing the resistance to the ingress of detrimental materials such as chloride and CO_2. The creep of concrete is able to reduce the prestressing force of prestressed concrete structures and leads to an increase of the deflection and reduction of the cracking load during service life. Even though these phenomena may not influence the ultimate capacity of concrete structures, the durability and serviceability of such structures can be decreased. Hence, an accurate prediction of long-term shrinkage and creep deformation under actual outdoor environmental conditions is of great importance from the view of rational design as well as the construction of high quality infrastructures.

Since shrinkage and creep are greatly affected by surrounding environmental conditions, numerous laboratory studies of these behaviors focusing on ambient temperature and relative humidity have been reported. On the other hand, a few studies have also reported the behavior of creep and shrinkage under varying actual environments [1–6]. The comprehensive examination of the influence of actual environmental conditions such as solar radiation and rain on shrinkage and creep of concrete can make the effective prediction of the degradation of each structure member possible, since large civil infrastructures can have numerous members that are subject or not subject to solar radiation and rain.

It is easily anticipated that the increase of temperature in concrete due to solar radiation can accelerate shrinkage and creep with the drying of internal pores, while rain makes pores saturated due to infiltration of rain water to reduce shrinkage and creep. However, the acceleration and inhibition effects arising from solar radiation and rainfall have not been quantitatively understood so far. Furthermore, shrinkage cracking is likely to be promoted by the increase of the shrinkage under solar radiation but is also possible to be inhibited if the tensile creep can be increased at hot temperature due to solar radiation as the compressive creep is increased with the surrounding temperature rise [7], while it was found that the smaller tensile creep of concrete with lower W/C cannot release the restraint and is able to cause shrinkage cracking earlier [8]. As El-Sakhawy et al. [9] experimentally reported that the repeated cycle of wetting and drying can reduce the tensile strength, solar radiation drying and rain wetting cycle is plausible to decrease the strength and to promote shrinkage cracking. As mentioned above, the influence of the actual environment on shrinkage, creep and shrinkage cracking is complicated and remains uncertain, and accordingly the effects of solar radiation and rain have not yet been implemented in design codes.

In this paper, the authors endeavor to study the effects of solar radiation and rain on concrete shrinkage, shrinkage cracking, and

* Corresponding author. Tel./fax: +81 48 858 3556.
E-mail address: asamoto@mail.saitama-u.ac.jp (S. Asamoto).

Table 1
Mix proportion, compressive strength, and Young's modulus of concretes. (Shrinkage and shrinkage cracking tests).

W/C	Water [kg/m³]	Cement [kg/m³]	Fine aggregate [kg/m³]	Coarse aggregate [kg/m³]	Compressive strength [N/mm²]	Young's modulus [kN/mm²]
55.0%	170	309	819	975	39.4	32.5
30.0%	170	567	751	901	59.2	36.0

Cement: Ordinary Portland cement (specific gravity: 3.15), fine aggregate: river sand (specific gravity: 2.59; water adsorption: 2.53%), coarse aggregate: sandstone (specific gravity: 2.65; water adsorption: 0.70%).

creep consistently. The shrinkage and creep behavior of plain concrete under drying conditions with or without solar radiation and rain is explicitly investigated. The shrinkage cracking behavior using concrete with a large amount of reinforcement is also examined. Two types of concrete with different water-to-cement ratios are compared to evaluate the effect of mix proportion. In the paper, firstly moisture loss and shrinkage behavior of plain concrete under each drying condition are discussed and then shrinkage cracking behavior of reinforced concrete is studied based on the shrinkage behavior of plain concrete. Finally, the effects of solar radiation and rainfall on specific creep of plain concrete are examined.

2. Experimental program

2.1. Test specimens

2.1.1. Shrinkage and shrinkage cracking tests

The shrinkage test of plain concrete and the shrinkage cracking test using reinforced concrete were carried out to study shrinkage and shrinkage cracking behaviors under outdoor conditions. Two mix proportions with the same water content were studied, as shown in Table 1. The type of cement used was Ordinary Portland Cement (Type I Portland Cement). The compressive strength and Young's modulus in Table 1 were obtained by compressive test using φ100×200 mm cylinder specimens after 28 days of moist curing.

Two prismatic specimens of plain concrete with dimensions 100×100×400 mm (with high surface area/volume S/V = 0.045 mm⁻¹) and 100×200×200 mm (with lower S/V = 0.01 mm⁻¹) were used for the shrinkage test. All of surfaces of the 100×100×400 mm specimens were untreated, while the 100×200×200 mm specimens were coated with epoxy to prevent moisture transfer and then with heat insulation material to impede heat transfer on all the surfaces, apart from two opposing 100 mm×200 mm faces, as shown in Fig. 1.

Prismatic specimens with a dimension of 100×100×1000 mm embedding a large steel reinforcement bar of 32 mm in diameter (reinforcement ratio: 8.04%) in the center of the cross section, as to provide a significant restraint of shrinkage, were used for the shrinkage cracking test. The minimum of bond length between concrete and steel for a straight tensile reinforcement of RC structure is specified in each design code. According to JSCE [10], the length can be calculated depending on strengths of concrete and steel, the bar

radius and others and should be at least longer than twenty times of the bar diameter. In our experimental conditions, the length is determined to be 640 mm in both W/C, because the calculated values associated with the properties of concrete and steel are smaller than 640 mm. Hence, the total bond length in the specimen needs at least 1280 mm, when it follows the specification of the bond length for tensile reinforcement. This bond length, however, is for the tensile reinforcement that can transfer the bond stress between concrete and steel until the yielding point of the steel and appears to be much long to transfer small shrinkage stress in the experiment. Indeed, Nakagawa and Ohno [11] investigated the strain distribution of the embedded steel bar of 32 mm in diameter in the sealing concrete specimen with a 100×100 mm cross section and W/C of 0.24 at early ages. It was found that the bond between the concrete and the reinforcement can be enough to transfer shrinkage stress in concrete if the bond length at both ends is more than 300 mm. Thus, in the shrinkage cracking test, the longitudinal length of the RC specimen was set to 1000 mm as small as possible to have sufficient bond to induce the shrinkage cracks over the specimen.

The casting was carried out in September 2007 when it is summer in Japan and the moist curing wrapped by wetting waste clothes was conducted for all specimens for 2 days after removing the form at 1 day of age. After three days of initial curing, the specimens were dried under three different outdoor conditions that will be explained in Section 2.2.

The longitudinal length change of about 100 mm spans in specimens of shrinkage and shrinkage cracking tests were measured by using a contact strain gauge with an accuracy of 0.001 mm. The length changes of the two 100×100×400 mm and 100×100×1000 mm sides and those of the top and bottom of the 100×200×200 mm specimens (the top is the casting surface) were measured and averaged. In the paper, the relative length change to the initial length after curing subtracting a thermal strain is defined as a shrinkage strain. The weights of plain concrete specimens were also measured with a resolution of 1 g after curing and during drying in order to determine the amount of water that evaporated from the specimens. In the case of the 100×100×400 mm specimens, the results of shrinkage and moisture loss under each drying condition were the mean values of the two specimens. In the case of the 100×200×200 mm and 100×100×1000 mm specimens, results under each drying condition were obtained from one specimen. The interior temperature of all specimens and the top surface temperatures of the 100×200×200 mm specimens were measured by a thermocouple. At the beginning of the drying, the weight and the shrinkage were measured frequently, while the measurement after 120 days of drying when the variation was smaller was conducted at about 2 month intervals. They were measured when it did not rain to avoid the sudden weight increase or swelling due to rain water infiltration during measurement. Table 2 summarizes the specimen size, number of the specimens, and measurement items including creep test described in the next session and Fig. 2 gives the schematic representation of the specimens for the shrinkage and shrinkage cracking tests.

2.1.2. Creep test

The creep test was started at a different time from shrinkage and shrinkage cracking tests due to space and time limitation. The creep test is independent of the shrinkage and shrinkage cracking tests in the
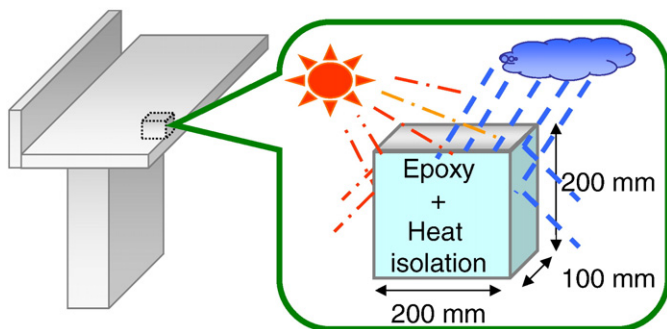

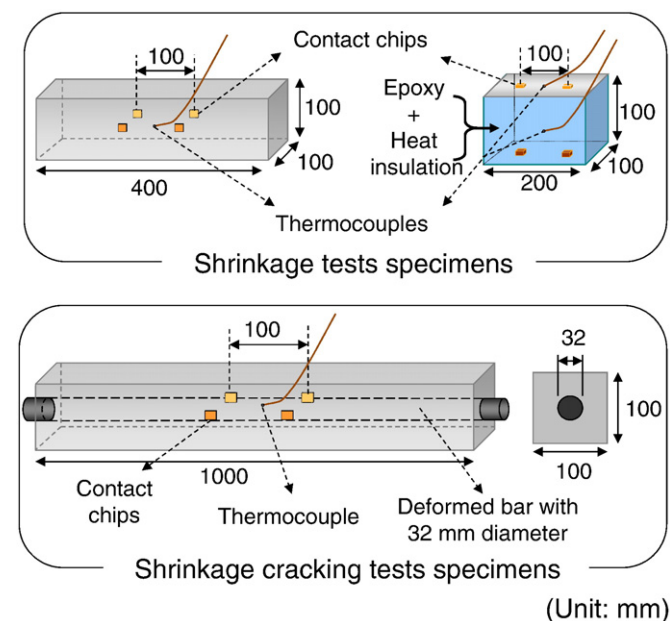**Fig. 1.** 100×200×200 mm specimen.

Table 2
Specimen size, number of specimens and measurement items of all tests.

Test	Specimen size	Number of specimens under each condition	Measurement items
Shrinkage test	$100 \times 100 \times 400$ mm	2	i. Weight ii. Shrinkage strain by contact strain gauge iii. Internal temperature
	$100 \times 200 \times 200$ mm	1	i. Weight ii. Shrinkage strain by contact strain gauge iii. Internal and surface temperature
Shrinkage cracking test	$100 \times 100 \times 1000$ mm	1	i. Shrinkage strain by contact strain gauge ii. Number of shrinkage cracks by visual and microscope observation iii. Internal temperature
Creep test (Loaded specimens and shrinkage specimens)	$100 \times 100 \times 400$ mm with center hole of 32 mm	2	i. Longitudinal strain by electric strain gauge ii. Internal temperature

paper and the different types of the cement and coarse aggregate from those of the previous tests were used, though the same water content and W/C were adopted, as shown in Table 3. The type of cement was High-early-strength Portland Cement (Type III Portland Cement) to provide prestress at 3 days of age (an early age) as do in actual prestressed concrete structures and the coarse aggregate was crushed limestone. The compressive strength and Young's modulus in Table 3 were also obtained by using $\phi 100 \times 200$ mm cylinder specimens after 28 days of moist curing. $100 \times 100 \times 400$ mm prismatic specimens containing a PVC pipe with an outer diameter of 32 mm and an inner diameter of 25 mm to pass pre-stressing tendons were used for the loaded specimens. In order to apply a sustained compressive stress in the longitudinal direction, steel plates of about 15 mm thick having a hole in the center were attached at both ends and a prestressing steel bar of 17 mm in diameter was inserted through the pipe without grouting. In order to obtain the creep strain that is calculated by subtracting the shrinkage strain and the elastic strain due to the prestressing from the total longitudinal strain of the loaded specimen, shrinkage of the non-loaded specimens with the same dimension having the pipe without load was measured at the same time. Both ends of the shrinkage specimens were sealed with aluminum tape to make the boundary conditions the same as those of the loaded specimens. Fig. 3 shows the schematic representation of the loaded and non-loaded shrinkage specimens for creep test.

The casting was carried out in August 2008 about one year after the start of the shrinkage tests and moist curing by wetting waste clothes was conducted for all specimens for 2 days, as well as the shrinkage tests. A sustained compressive load was applied to the specimens by hand fastening the prestressing steel bar with nuts. The applied stress was calculated by checking the average strain value obtained from two 2 mm foil electric strain gauges in the center of the bar as shown in Fig. 3. The applied stresses were approximately 20% (3.6 N/mm^2) and 15% (8.0 N/mm^2) of the compressive strength of concrete with W/C$=0.55$ and 0.30 after the curing, respectively. After the stress was applied, the specimens were exposed to the same three different conditions as those in shrinkage tests and the longitudinal strain of concrete was measured using 3 cm polyester foil electric strain gauges on the two sides' surfaces in the center as given in Fig. 3. Whenever about 10% reduction of the initial applied stress was observed due to creep and shrinkage in the loaded specimens, the load was applied again to reach the initial applied stress. The elastic strain due to each prestressing as well as shrinkage strain was subtracted from the total strain of the loaded specimen to obtain the creep strain. Since the thermal coefficient of the concrete cast at different times with the same mix proportion was measured to be 7.4 μ/°C which is much smaller than that of the strain gauge with 11 μ/°C, the thermal strain difference arising from temperature variation was subtracted from the measured strain by the strain gauge, using internal temperature by thermocouples. The results were the mean values for the two specimens and the test information is also summarized in Table 2.

2.2. Environmental conditions

In order to study the effects of solar radiation and rain on shrinkage, shrinkage cracking and creep of concrete comprehensively, three artificial outdoor drying conditions were set up. Table 4 summarizes the drying conditions in the test program. The specimens were stored at a height of about 1.2 m from the ground to exclude the effect of heat on the ground, based on the WMO specification of temperature measurement [12]. Under condition SR, the specimens were exposed to the wetting and drying cycle arising from the actions of rain and solar radiation. On the other hand, rain and solar radiation were blocked under condition N using the wooden well-ventilated cage like a thermometer shelter, as shown in Table 4. Condition S where clear plastic roof and wall with gaps can prevent rain and allow solar radiation and wind is expected to be in the most severe drying condition because the solar radiation promotes drying without rain. For reference, other specimens were dried in a well-controlled chamber of a relative humidity of 60% and 20 °C.

The ambient temperature and relative humidity measured data by the Ministry of Environment [13] in the place about 800 m from the laboratory were used for reference, while the amount of rainfall in the city where the laboratory is located was obtained from the Japan Meteorological Agency [14]. During shrinkage and shrinkage cracking

Fig. 2. Schematic representation of specimens for shrinkage and shrinkage cracking tests.

Table 3
Mix proportion, compressive strength, and Young's modulus of concretes. (Creep tests).

W/C	Water [kg/m^3]	Cement [kg/m^3]	Fine aggregate [kg/m^3]	Coarse aggregate [kg/m^3]	Compressive strength [N/mm^2]	Young's modulus [kN/mm^2]
55.0%	170	309	815	993	26.1	29.5
30.0%	170	567	753	918	63.2	40.9

Cement: High-early-strength Portland cement (specific gravity: 3.14), fine aggregate: river sand (specific gravity: 2.60; water adsorption: 1.94%), coarse aggregate: limestone (specific gravity: 2.70; water adsorption: 0.39%).

tests, the mean temperature and relative humidity were 14.6 °C and 63.3%, respectively. In the case of creep test, the mean temperature and relative humidity were 16.4 °C and 64.9%, respectively. Fig. 4 shows the variation of ambient temperature and relative humidity during the shrinkage and creep tests.

3. Experimental results and discussion

3.1. Effects of solar radiation and rain on moisture loss behavior of concrete

The variation of the loss of mass of the specimens with dimensions $100 \times 100 \times 400$ mm is given in Fig. 5. The loss of mass was calculated by dividing the weight difference between the dried specimen and the cured specimen by the weight of the cured specimen. The loss of mass of specimens with W/C = 0.55 under condition N suddenly decreased due to the leakage of rain from a part of the roof at 180 days of drying time. However, since the loss of mass was increased after repairing the roof and the tendency could be similar to that in the case of specimens with W/C = 0.30, the influence of this leakage is regarded as small. Under all conditions, the moisture loss of concrete with W/C = 0.30 was much less than that of concrete with W/C = 0.55. This is ascribed to lower porosity of lower water-to-cement ratio concrete as a previous study pointed out [15].

Comparing moisture behaviors under condition S with solar radiation and condition N without solar radiation, the loss of mass of the concrete under condition S was about 50% larger than that under condition N in the cases of both low and high W/C because solar radiation raises the temperature of the concrete and causes the drying to accelerate. The temperature rise due to solar radiation will be described in Section 3.3.

Next, the influence of rain on moisture loss is discussed by comparing moisture behavior under condition SR with rain to that under condition S without rain as shown in Fig. 5. In the beginning of the drying process, the penetration of liquid rain water greatly reduced the loss of mass of the concrete under condition SR, while the ingress of vapor in the air did not decrease the loss of mass of the concrete much in the case of condition S, even though the ambient relative humidity increased due to the rain. The loss of mass of the concrete under condition SR showed only a slight increase from 50 to 80 days of drying time when there were few rainy days in winter of Japan even if condition SR includes solar radiation. The tendency is the same between both the low and high water cement ratios. It was concluded that rain can greatly inhibit moisture loss and once rainwater directly penetrates the internal pores of concrete a long time is needed for the moisture to evaporate and the loss of mass remains small.

In addition, the loss of mass under condition SR from 80 to 200 days of drying time when there were many rainy days without heavy rain in the rainy season of Japan remained almost the same because the continuous rainwater was gradually absorbed into the inside of the concrete. As Andrade et al. [16] indicated, the penetration of rainwater is affected more by the duration of the rainy period than by the amount of rain that falls.

The variation in the loss of mass of the specimens with the dimensions of $100 \times 200 \times 200$ mm is shown in Fig. 6. It is plausible that the heat insulation material absorbs rain water but should be dried soon under fine weather due to its rough porous media. In fact, when the heat insulation material was submerged into water for one day and then dried in the laboratory for one day, more than 99% of the absorbed water evaporated. In addition, the absorbed water in the heat insulation material could not penetrate into concrete because the sides of the
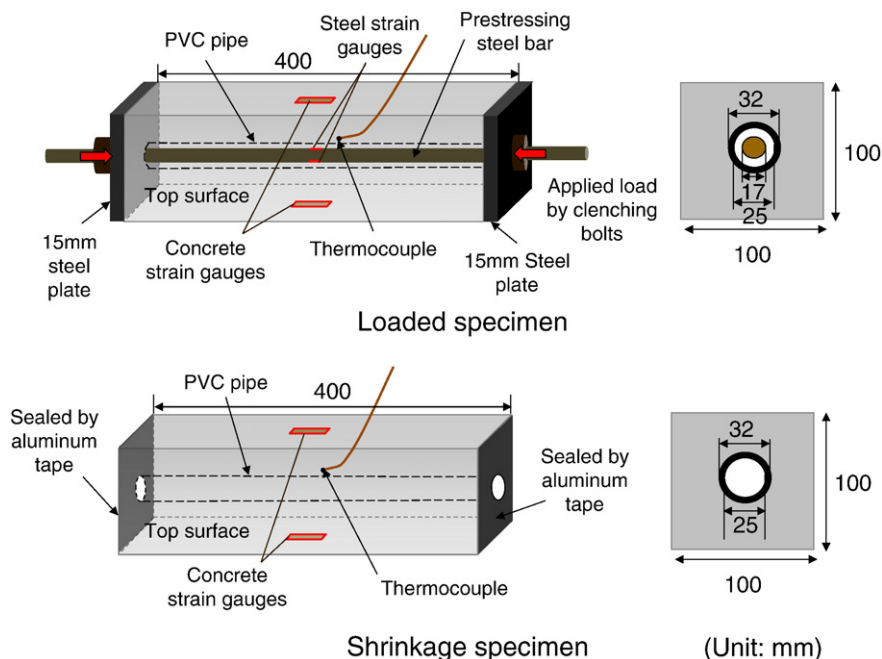

Fig. 3. Specimens for creep tests.

Table 4
Summary of each drying condition.

Condition	Solar radiation	Rain	Exposure conditions
C	No	No	Controlled chamber with 20 °C, 60% relative humidity
S	Yes	No	
N	No	No	
SR	Yes	Yes	

concrete with the insulation material were coated by sufficient epoxy resin. Though the water absorption of the heat insulation might affect the weight measurement of the specimen, the influence on the loss of mass should be small because the measurement was conducted when it did not rain and the concrete could not absorb rain water from the sides due to the epoxy protection.

The negative values of the loss of mass of the specimens under condition SR in the beginning of the drying process could be affected by the rain penetration into the self-desiccated concrete from the top of the specimen, while other specimens under conditions S and N without rain decreased the weights continuously. The loss of mass of the concrete under condition S was not much different from that under condition N, while the moisture loss under condition S was greater than that under condition N in the case of the $100 \times 100 \times 400$ mm specimens. This is attributed to the smaller ratio of the surface area exposed to solar radiation to the total drying surface. In the case of specimens with a smaller S/V that is a possible value in the actual civil structure, rain can

also significantly inhibit drying and lead to the smallest loss of mass under condition SR. It is inferred that rain can interfere with the drying process in the case of actual concrete structures and that absorbed rainwater is unlikely to evaporate even under solar radiation.

The larger increase in the rate of the loss of mass after 180 days appears to be caused by a gradual loss of part of the heat insulation material on the sides due to long-term exposure to the environment. Since the tendencies of moisture loss under each condition after 180 days are not different from those during the first 120 days when the heat insulation might not be damaged, it appears that the influence of the loss of heat insulation material should not be significant but the accuracy of the latter data of the loss of mass after 180 days is not guaranteed.

3.2. Effect of solar radiation and rain on shrinkage behavior of plain concrete

The variations of the shrinkage of the $100 \times 100 \times 400$ mm concrete specimens under each condition are represented in Fig. 7. Here, the thermal coefficient was assumed to be 10 μ/°C that was measured using the specimens cast at different times with the same mix proportion and the shrinkage strains were obtained by subtracting the thermal strain using the measured internal temperature from the measured relative length change.

The influence of the water-to-cement ratio, within the range from 0.30 to 0.55, on the drying shrinkage under every condition was found to be small as suggested in a previous study [17], while the moisture loss of the concrete with W/C = 0.55 was much larger than that of the concrete with W/C = 0.30. Since the curing period in the experiment was relatively short, the large autogenous shrinkage due to a continuous hydration reaction in the case of low W/C concrete can occur with drying shrinkage and lead to the same amount of total shrinkage as that of the W/C = 0.55 concrete, which has more drying shrinkage but less autogenous shrinkage as analytically indicated in a previous research [18].

Next, the effects of the storage conditions are discussed. By examining the experimental results shown in Fig. 7, it appears that shrinkage behavior is scarcely influenced by solar radiation because the shrinkage under condition N without solar radiation was close to that of condition S with solar radiation even though the loss of mass under condition N was greater than that under condition S, as shown in Fig. 5. The reason for this behavior will be discussed later in this section. The
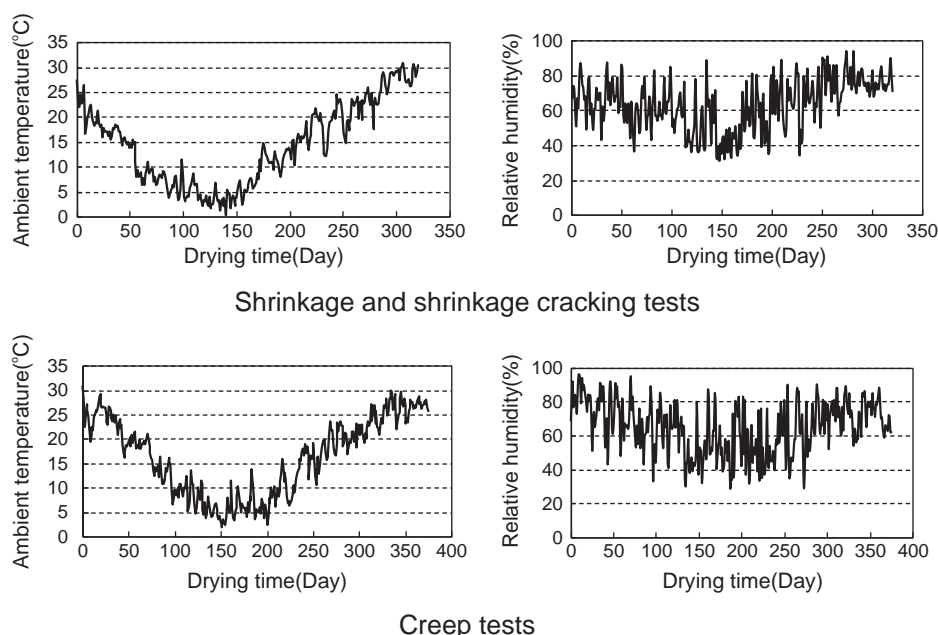

Shrinkage and shrinkage cracking tests

Creep tests

Fig. 4. Variation of ambient temperature and relative humidity during tests.
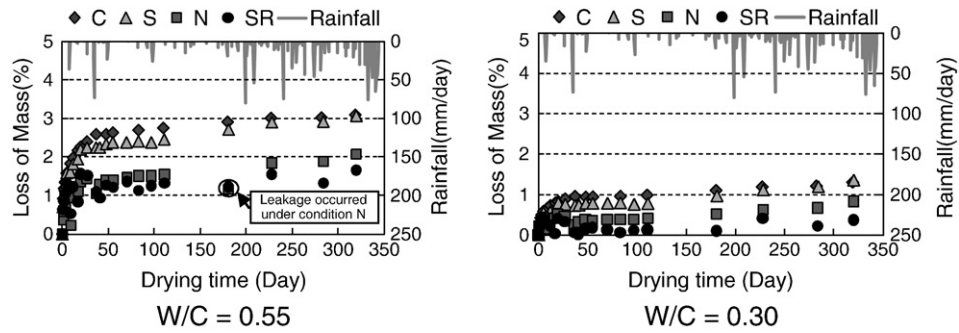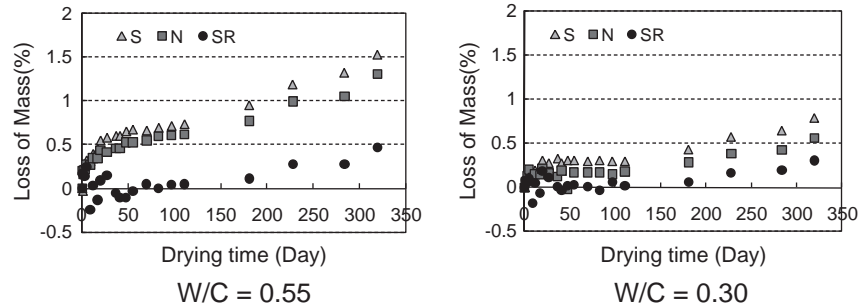
Fig. 5. Variation in loss of mass ($100 \times 100 \times 400$ mm specimens).

Fig. 6. Variation of loss of mass ($100 \times 200 \times 200$ mm specimens).
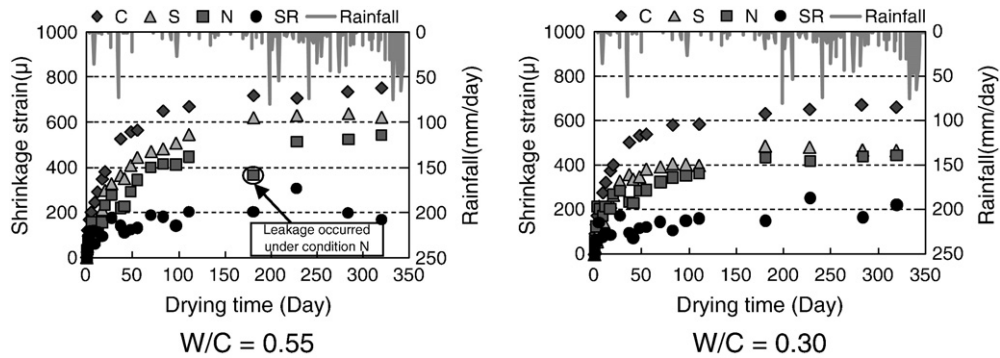

Fig. 7. Variation of shrinkage ($100 \times 100 \times 400$ mm specimens).

shrinkage under condition SR with both solar radiation and rain was always the smallest. It is indicated that rain greatly inhibits the shrinkage behavior of concrete as does moisture loss. In practical design, the average ambient relative humidity is considered as a significant parameter but the results indicate that rain should also be considered because the shrinkage under condition SR significantly

recovered due to penetration of rain water into concrete and remained small even when it was fine after rain, while the shrinkage under conditions S and N without rain increased continuously with drying.

The shrinkage behavior of the $100 \times 200 \times 200$ mm specimens shows almost the same tendency as that of the $100 \times 100 \times 400$ mm specimens even if S/V is small like actual concrete structures, as shown in Fig. 8. In
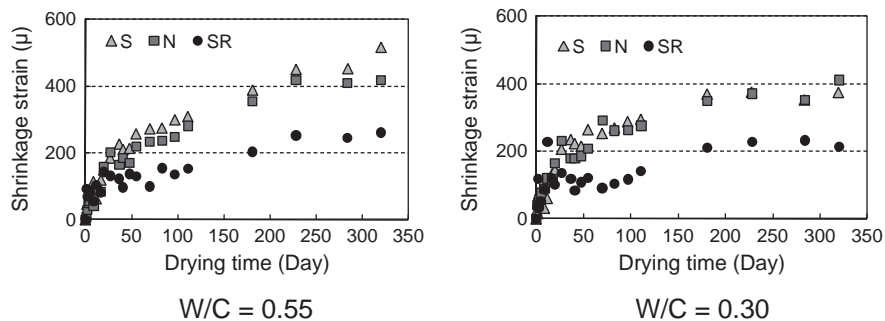

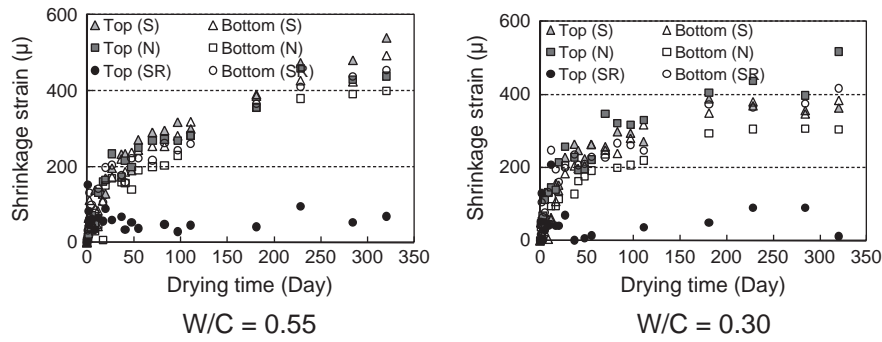**Fig. 8.** Variation of shrinkage ($100 \times 200 \times 200$ mm specimens).

Fig. 9. Shrinkage strains on top and bottom surfaces (100×200×200 mm specimens).

Fig. 9, changes in the shrinkage of the top surface and the bottom surface of the 100×200×200 mm specimen under each condition are represented. The shrinkage of the top surface with rain under condition SR was significantly smaller than that of the top surface under other conditions without rain. On the other hand, the shrinkage of the bottom surface, which was not subject to solar radiation and rain, was not much different among all conditions. Since the shrinkage shown in Fig. 8 is the average of the shrinkage of the top and bottom surfaces, the shrinkage under condition SR is the smallest due to the greatly inhibited shrinkage of the top surface by the presence of rain. The inference of these results is that the shrinkage of the concrete on the surface of the slab that is exposed to rain could be greatly impeded and the shrinkage cracking might be reduced more than that on the bottom surface which is not exposed to rain.

Next, the experimental results under each condition are compared with the prediction model of the JSCE design codes [10]. Here, only the results of concrete with W/C=0.55, so-called conventional normal strength concrete, are used for the comparison because the shrinkage tendency of concrete with lower W/C is the same under each condition as that of normal strength concrete. The JSCE prediction model for the shrinkage of normal strength concrete is described as below,

$$\varepsilon'_{cs}(t, t_0) = \left[1 - \exp\left\{-0.108(t-t_0)^{0.56}\right\}\right] \times \varepsilon'_{sh}$$
$$\varepsilon'_{sh} = -50 + 78[1 - \exp(RH/100)] + 38\,lnW - 5[\,ln(V/S/10)]^2 \tag{1}$$

where, ε'_{sh}: final value of shrinkage strain [×10⁻⁵], ε'_{cs}: shrinkage strain between ages t_0 and t [×10⁻⁵], RH: ambient relative humidity [%], W: unit content of water [kg/m³], V: volume [mm³], S: surface area in contact with air [mm²], and t_0 and t: temperature adjusted age

[days] of concrete at the beginning of drying and during drying, where the value corrected by Eq. (2) should be used.

$$t_0 \text{ and } t = \sum_{i=1}^{n} \Delta t_i \times \exp\left[13.65 - \frac{4000}{273 + T(\Delta t_i)/T_0}\right] \tag{2}$$

where, Δt_i: number of days when the temperature is T, $T(\Delta t_i)$: the temperature during the time period Δt_i [°C], and T_0: 1 °C. The material variables used in the model are the same as the mix proportion and the specimen size. The daily temperature variation was taken into account in Eq. (2) and the average relative humidity was used referring to the Ministry of Environment [13].

The comparison between experimental and predicted results of the shrinkage of the 100×100×400 mm and the 100×200×200 mm plain concrete specimens is given in Fig. 10. Although the shrinkage of both different specimens under conditions S and N is almost predicted well by the model, the prediction greatly overestimates the shrinkage under condition SR. The prediction model is identified based on numerous laboratory experimental tests where specimens are not subjected to solar radiation and rain like condition N. Hence, as discussed above, it is also suggested that the shrinkage of the concrete exposed to rain could be smaller than the expected while the shrinkage of the concrete without rain, even if subjected to solar radiation, can be predicted reasonably.

The relationships between the loss of mass and shrinkage are shown in Fig. 11. Comparing the relationship between conditions S and N without rain, shrinkage at the same loss of mass is quite different. The difference suggests that the shrinkage of the concrete is likely to be affected not only by the loss of moisture but also by the drying rate. Recently, Maekawa et al. [19] proposed a multi-scale constitutive model that can simulate concrete time-dependent behavior such as shrinkage and creep based on the hydration reaction, pore structure and moisture
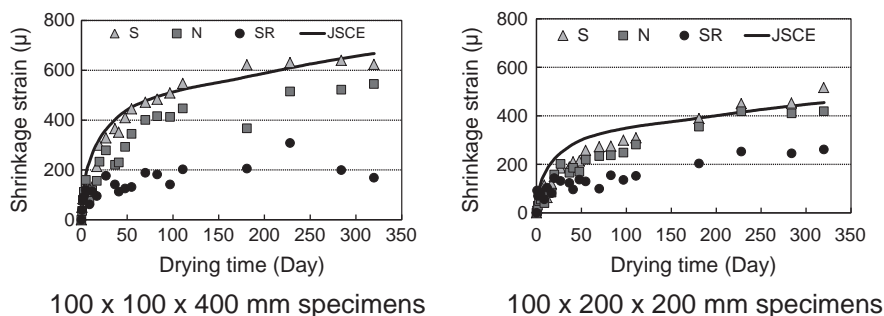

Fig. 10. Comparison of measured shrinkage strains with JSCE model predictions (W/C=0.55).
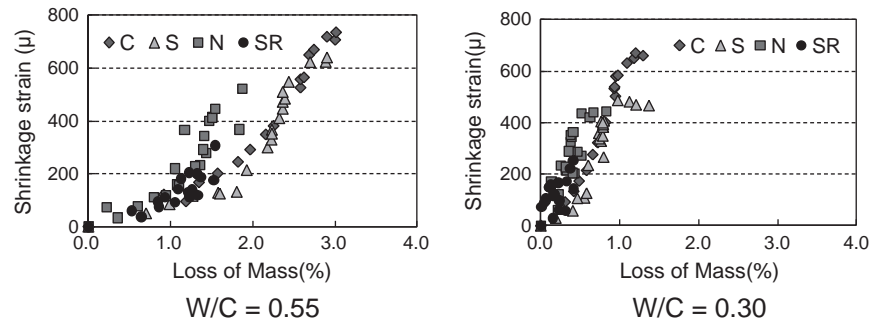
Fig. 11. Relationship between shrinkage strain and loss of mass ($100 \times 100 \times 400$ mm specimens).

state in the pores. According to the model, the shrinkage can be expressed to be a total strain by summing up elastic strain and accumulated time-dependent strain due to the varying shrinkage stress depending on moisture states in pores without external stress. It is suggested that severer drying condition may provide smaller time-dependent deformation and results in smaller shrinkage at the equivalent moisture loss than gradual drying does because it has shorter time to reach the same moisture loss under severer drying. Thus, since drying under condition N seems to be more promoted due to solar radiation in comparison with condition S, the same interpretation according to their model can be accepted for our experimental results. Moreover, it is also plausible that more microcracks in concrete can form under the severest cyclic temperature loading and drying conditions of condition S with solar radiation and without rain, especially in summer, as the previous study suggested [9] and reduce the apparent measured shrinkage. Since the authors currently do not have sufficient information to profoundly discuss the above deductions, however, further detailed investigation into the effect of drying rate on the shrinkage is necessary.

3.3. Effect of solar radiation and rain on shrinkage and shrinkage cracking behavior of reinforced concrete

The results of the shrinkage of reinforced concrete specimens with a cross section of 100×100 mm and a length of 1000 mm are given in Fig. 12. The number of shrinkage cracks of the specimens at each drying time is listed in Table 5. Although the cracks were observed visually up to 280 days, at 280 days, the cracks were also examined by using a digital microscope.

The shrinkage strain of concrete with W/C = 0.30 under condition S gradually decreased after 20 days of drying, while the shrinkage of plain concrete increased continuously, as shown in Figs. 7 and 8. This appears to be because shrinkage cracks first occurred on the surface of the specimens after around 20 days drying and propagated gradually. The surface cracks cause the internal stress and strain to be discontinuous and lead to a decrease of the apparent measured

shrinkage on the surface. In the case of specimens with W/C = 0.55, it seems that less and finer shrinkage cracks are not enough to greatly reduce the shrinkage even under condition S.

There were more shrinkage cracks of the RC specimen having a low water-to-cement ratio under all conditions than were those of the specimen with W/C = 0.55, while the shrinkage of plain concrete was not much distinct between those with different water-to-cement ratios. This is speculated to be due to a stronger bond between concrete and reinforcement in the case of concrete with a lower W/C and more shrinkage cracks develop due to the stronger confinement caused by the reinforcement even if the same amount of concrete shrinkage was exhibited. In addition, it also attributes to smaller shrinkage stress relaxation due to smaller tensile creep of concrete with lower W/C as suggested in a previous research [8].

An interesting finding from the experimental results is that a larger number of shrinkage cracks were generated under condition S than those under condition N, although the difference in the shrinkage of plain concrete under conditions S and N is less than 50 μ. This indicates that solar radiation accelerates the generation of shrinkage cracks.

Typical variations in the surface and internal temperatures of the specimens around when the first shrinkage cracks appeared are shown in Fig. 13. The surface temperature was measured on the surface of the $100 \times 200 \times 200$ mm specimen and the interior temperature was measured in the $100 \times 100 \times 1000$ mm specimen. Here, the surface temperature of the $100 \times 200 \times 200$ mm specimen is assumed to be the same as that of the $100 \times 100 \times 1000$ mm specimen because the surface temperature is considered independent of dimension but dependent on material properties. According to Fig. 13, since the difference in temperature between the surface and the inside of the specimen was less than 2 °C under both conditions S and N, the small gradient of thermal strains between the internal and surface arising from solar radiation has a small contribution to the generation of the shrinkage cracking. However, temperature variations during the day were significantly different between conditions S and N. Whereas the lowest
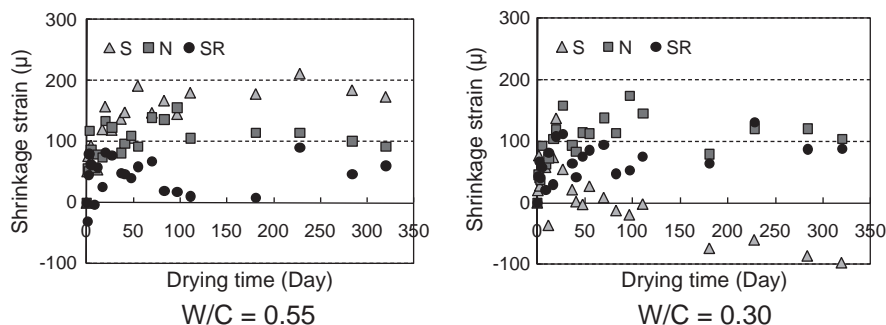

Fig. 12. Variation of shrinkage of reinforced concrete specimens ($100 \times 100 \times 1000$ mm specimens).

Table 5
Number of shrinkage cracks.

Condition	W/C	Drying time			Time initial cracks are observed
		110 days	180 days	280 days[*]	
S	0.55	6	12	12	55 days
	0.30	18	22	22	26 days
N	0.55	0	4	5	83 days
	0.30	1	8	8	55 days
SR	0.55	0	0	5	228 days
	0.30	0	0	9	280 days

[*] The cracks were observed by digital microscope at 280 days of drying time, while visual inspection was carried out in other cases.
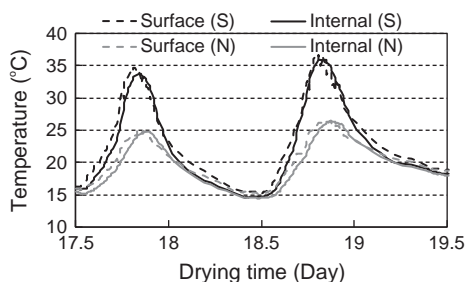
Fig. 13. Variation of surface and internal temperature under conditions S and N.

temperature at night was almost the same for conditions S and N, the highest temperature during the day under condition S was about 10 °C higher than that under condition N. El-Shakhawy et al. [9] indicated that the cyclic temperature due to summer sunlight and cool night can cause loss of inherent water and lead to internal stresses and cracking inside the concrete matrix. Thus, it is deemed that the reduction of concrete strength due to the degradation of the concrete matrix generates more shrinkage cracks under condition S than those under condition N where cyclic temperature is less severe.

Fig. 14 shows the ignition loss of the small samples crushed from the surface and center of the $100 \times 100 \times 400$ mm specimens of plain concrete for shrinkage test from 105 °C to 950 °C in a muffle furnace. Since the ignition loss primarily arising from the evaporation of bound water is able to represent the degree of hydration, the progress of the hydration reaction on the surface and in the center of the specimens can be compared based on the ignition loss. The ignition losses on the surface under conditions SR and S were the largest and the smallest among results on the surface, respectively, while those in the center were not so different under either condition. The tendency is the same in the cases of both low and high water-to-cement ratio concretes. The temperature rise due to solar radiation not only promotes the hydration reaction but also impedes the reaction because the water for the hydration reaction in the capillary pores evaporates fast at an elevated temperature. In the case of condition SR, the water can be provided in the unsaturated pores again because of the rain, while the pores are unlikely to be saturated under condition S without direct

penetration of liquid water. Thus, it is deduced that the lower chemical reaction of the concrete at the surface of RC specimens under condition S weakens the tensile strength of the surface concrete and engenders more shrinkage cracks than those in the case of conditions N and SR. On the other hand, since it can take a long time for the moisture in the pores at the center to disperse outside, the difference of the degree of hydration in the center due to evaporation of capillary water is small. Although the temperature rise due to solar radiation under conditions S and SR can accelerate the reaction as mentioned above, its effect appears to be relatively small.

Fig. 15 shows the crack width and the number of cracks at 280 days of drying time. The crack width was obtained by averaging the largest three crack widths in the captured digital image of the crack by using a digital microscope. The number of cracks under condition SR was almost the same as that under condition N, although the shrinkage of plain concrete under condition SR was much smaller than that in the case of condition N, and the crack width under condition SR was smaller. Savastano et al. [20] reported that the greater severity of a tropical environment can be attributed to a subsequent leaching of concrete under the action of rainwater and to the propagation of microcracks generated by the cyclic action of temperature and moisture. Although the climate in Japan is not tropical, it is suggested that the weather of hard rainfall and strong sunshine in summer could be similar to a tropical environment and promote the generation of microcracks on the surface of concrete exposed to condition SR, even though the concrete shrinkage was inhibited by rain.

3.4. Effect of solar radiation and rain on creep behavior of concrete

The variations of shrinkage and specific creep in creep test are shown in Figs. 16 and 17, respectively. The specific creep was obtained by dividing the creep strain as defined in Section 2.1.2 by the applied compressive stress in concrete calculated from the strain of the prestressing steel bar. The data from around 100 days to 200 days under outdoor conditions was missed due to data logger error but the latter data after 200 days could be recovered. The tendency that the smallest shrinkage was observed under condition SR with rainfall and the shrinkages under conditions N and S were similar is almost the same as those in Fig. 7, while the amount of shrinkage was smaller than that of concrete with the same unit water content but different cement and coarse aggregate. It is ascribe to the mix proportion with a coarse aggregate of limestone causing smaller shrinkage than in the case of concrete with a coarse aggregate of sandstone as reported previously [21,22] and High-early-strength Portland Cement providing faster hydration reaction to make autogenous shrinkage smaller after curing.

Fig. 17 shows that the specific creep of concrete with lower W/C was smaller under any conditions as is well-known. Unlike the results of shrinkage, in cases of concretes with both high and low W/Cs, specific creep under condition S was the largest while those under conditions N and SR were not so different. Since concrete creep is
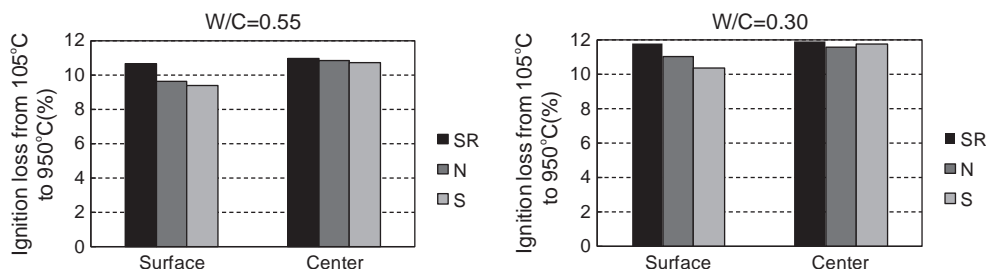

Fig. 14. Ignition loss of surface and center of $100 \times 100 \times 400$ mm specimens.
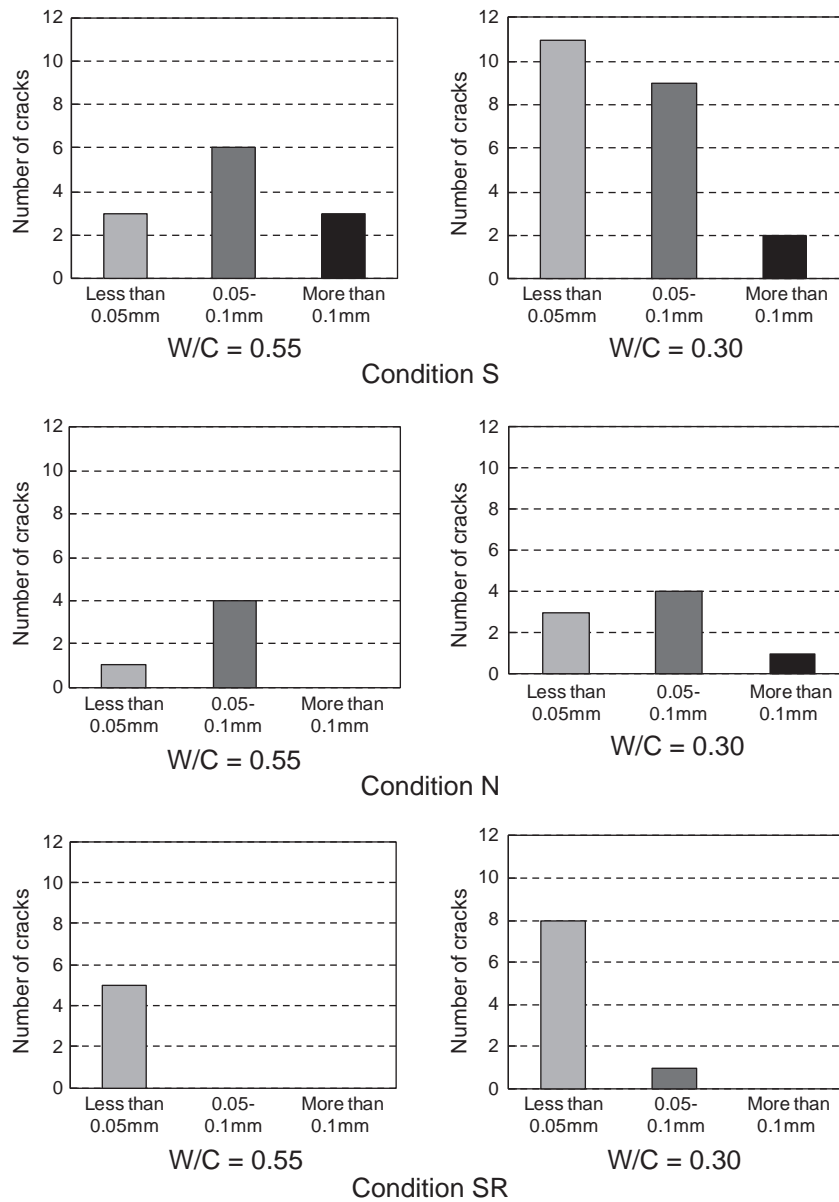
Fig. 15. Shrinkage crack width and distribution.

promoted at elevated temperatures [7], it is inferred that a local temperature rise in the daytime due to solar radiation under condition S, especially in summer, can increase the specific creep. Although condition SR can also accelerate creep owing to solar radiation, it is deduced that drying creep can be strongly inhibited by penetration of

rainwater and consequently the total creep becomes almost the same as that under condition N where neither acceleration nor inhibition effects on creep in the absence of solar radiation and rain.

The creep test results of normal strength concrete are also compared with the prediction by JSCE model [10] as well as shrinkage
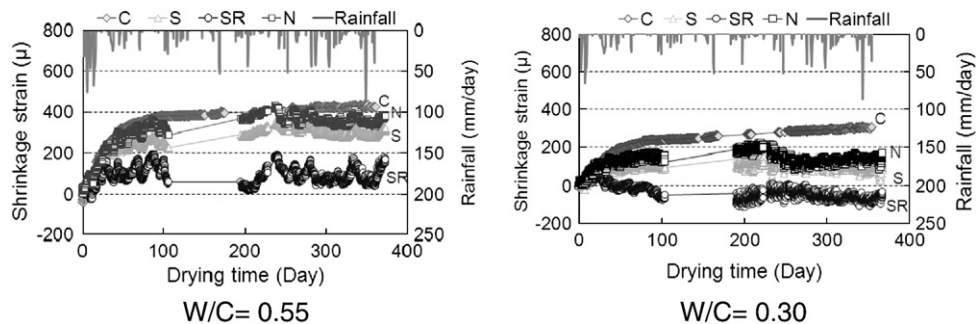

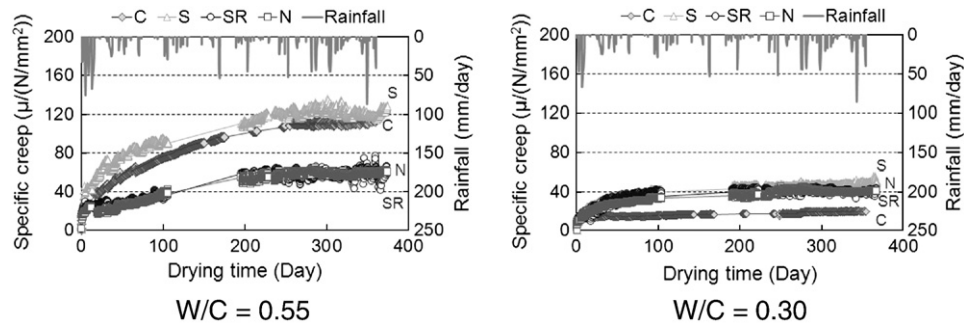**Fig. 16.** Variation of shrinkage of creep test specimens.

Fig. 17. Variation of specific creep of creep test specimens.

test. The specific creep under drying condition is expressed in JSCE design code as below.

$$\varepsilon'_{cc}(t,t',t_0)/\sigma'_{cp} = \left[1 - \exp\left\{-0.09(t-t')^{0.6}\right\}\right] \times \varepsilon'_{cr}$$
$$\varepsilon'_{cr} = \varepsilon'_{bc} + \varepsilon'_{dc}$$
$$\varepsilon'_{bc} = 15(C+W)^{2.0}(W/C)^{2.4}(\ln t')^{-0.67}$$
$$\varepsilon'_{dc} = 4500(C+W)^{1.4}(W/C)^{4.2}\left[\ln(V/S/10)\right]^{-2.2}(1-RH/100)^{0.36}t_0^{-0.30}.$$
$$(3)$$

ε'_{cr}: final value of creep strain per unit stress [$\times 10^{-10}$/(N/mm^2)], ε'_{bc}: final value of basic creep strain per unit stress [$\times 10^{-10}$/(N/mm^2)], ε'_{dc}: final value of drying creep strain per unit stress [$\times 10^{-10}$/(N/mm^2)], C: unit cement content [kg/m^3], W: unit content of water [kg/m^3], W/C: water-cement ratio, RH: ambient relative humidity [%], V: volume [mm^3], S: surface area in contact with air [mm^2], and t_0, t', and t: temperature adjusted age [days] of concrete at the beginning of drying, at the beginning of loading, and during drying, respectively; values corrected by Eq. (2) should be used. The material information was the same as written in Section 2.1.2 and the daily temperature variation and the average relative humidity were inputted as well as the way in Section 3.2.

Fig. 18 represents the comparison between the experimental results and predicted results by JSCE code. Even though the model is proposed based on laboratory experiments without rain and solar radiation such as condition N, the prediction greatly exceeds the specific creeps under all conditions. It is deemed that the limestone might decrease the specific creep as indicated in the previous study [21] and lead to the large overestimation of the measured specific creep, even the accelerated creep under conditions S. For more quantitative discussion of the prediction model applicability to actual conditions, the additional experiments such as to use concretes with different aggregates are necessary.

4. Conclusion

In this paper, a comprehensive experimental investigation into the effects of rain and solar radiation on shrinkage, shrinkage cracking,
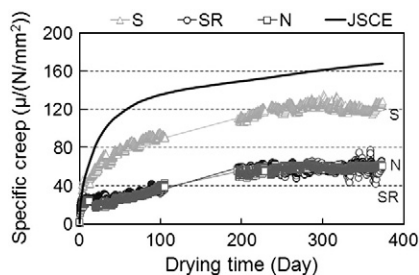

Fig. 18. Comparison of measured specific creep with JSCE model prediction (W/C=0.55).

and creep of concrete was carried out. It was found that the shrinkage of concrete is greatly inhibited by rainfall and that continuous rainy days can prevent the progress of shrinkage, even if the precipitation is small. The inhibition effect by rain on the moisture loss and shrinkage is greater than the acceleration effect due to solar radiation. Shrinkage cracking can be accelerated by solar radiation to promote the drying of the concrete surface and to decrease the degree of hydration related with the tensile strength. Since it was indicated that apparently the same shrinkage of plain concrete can cause different shrinkage cracking behaviors according to water-to-cement ratio and surrounding environment conditions, shrinkage cracking should be evaluated based on boundary conditions and mix proportion as well as the amount of plain concrete shrinkage. In addition, it was speculated that concrete creep can also be impeded by rain but be accumulated by the repeated temperature rise due to solar radiation in the daytime if the concrete is not subjected to rain.

Acknowledgement

References

[1] M.A. Mustafa, K.M. Yusof, Mechanical properties of hardened concrete in hot-humid climate, Cem. Concr. Res. 21 (1991) 601–613.
[2] K. Sakata, T. Ayano, Effect of temperature and relative humidity on concrete creep and shrinkage, Recent Advances in Concrete, ACI SP-179, 1998, pp. 1043–1058.
[3] B.I.G. Barr, J.L. Vitek, M.A. Beygi, Seasonal shrinkage variation in bridge segments, Mater. Struct. 30 (1997) 106–111.
[4] I.N. Robertson, Correlation of creep and shrinkage models with field observations, Am. Concr. Inst. Spec. Publ. 194 (2000) 261–282.
[5] B. Barr, S.B. Hoseinian, M.A. Beygi, Shrinkage of concrete stored in natural environments, Cement Concr. Compos. 25 (2003) 19–29.
[6] N.U. Kockal, F. Turker, Effect of environmental conditions on the properties of concretes with different cement types, Constr. Build. Mater. 21 (2007) 634–645.
[7] A.M. Neville, Properties of Concrete, fourth edition, 1995.
[8] T. Ohno, T. Uomoto, Prediction of cracks caused by autogenous shrinkage and drying shrinkage, Concr. Libr. Int. (38) (2001) 137–156.
[9] N.R. El-Sakhawy, H.S. El-Dien, M.E. Ahmed, K.A. Bendary, Influence of curing on durability performance of concrete, Mag. Concr. Res. 51 (1999) 309–318.
[10] Japan Society of Civil Engineers, JSCE Guidelines for Concrete No. 3 Standard Specifications for Concrete Structures − 2002 Structural Performance Verification, 2002.
[11] T. Nakagawa, Y. Ohno, Investigation of test method of self stress due to autogenous shrinkage in concrete, Proc. Jpn Concr. Inst. 20 (2) (1998) 751–756, (In Japanese).
[12] World Meteorological Organization HP, Measurement of temperature, http://www.wmo.int/pages/prog/www/IMOP/publications/CIMO-Guide/CIMO_Guide-7th_Edition-2008.html.
[13] Atmosphere information in Saitama, http://www.taiki-kansi.pref.saitama.lg.jp/ (In Japanese).
[14] Japan Meteorological Agency HP, http://www.jma.go.jp/jma/index.html (In Japanese).

[15] M. Azenha, K. Maekawa, T. Ishida, R. Faria, Drying induced moisture losses from mortar to the environment, I experimental research Mater. Struct. 40 (2007) 801–811.
[16] C. Andrade, J. Sarria, C. Alonso, Relative humidity in the interior of concrete exposed to natural and artificial weathering, Cem. Concr. Res. 29 (1999) 1249–1259.
[17] B. Bissonnette, P. Pierre, M. Pigeon, Influence of key parameters on drying shrinkage of cemetitious materials, Cem. Concr. Res. 29 (1999) 1655–1662.
[18] T. Ishida, R. Chaube, T. Kishi, K. Maekawa, Micro-physical approach to coupled autogenous and drying shrinkage of concrete, Concr. Libr. JSCE (33) (1999) 71–82.

[19] K. Maekawa, T. Ishida, T. Kishi, Multi-Scale Modeling of Structural Concrete, Taylor and Francis, 2008.
[20] H. Savastano Jr., P.G. Warden, R.S.P. Coutts, Potential of alternative fibre cements as building materials for developing areas, Cement Concr. Compos. 25 (2003) 585–592.
[21] G.E. Troxell, J.E. Raphael, R.W. Davis, Long-time creep and shrinkage tests of plain and reinforced concrete, Proceeding ASTM 58 (1958) 1101–1120.
[22] K. Imamoto, M. Arai, Simplified evaluation of shrinking aggregate based on BET surface area using water vapor, J. Adv. Concr. Technol. 6 (1) (2008) 69–76.